Deficient Ghrelin Receptor-mediated Signaling Compromises Thymic Stromal Cell Microenvironment by Accelerating Thymic Adiposity[*]

Yun-Hee Youm[‡], **Hyunwon Yang**[‡], **Yuxiang Sun**[§], **Roy G. Smith**[§], **Nancy R. Manley**[¶], **Bolormaa Vandanmagsar**[‡], **and Vishwa Deep Dixit**[‡1]

From the [‡]*Laboratory of Neuroendocrine-Immunology, Pennington Biomedical Research Center, Louisiana State University System, Baton Rouge, Louisiana 70808, the* [§]*Huffington Center on Aging, Baylor College of Medicine, Houston, Texas 77030, and the* [¶]*Department of Genetics, Coverdell Center for Biomedical and Health Sciences, University of Georgia, Athens, Georgia 30602*

With progressive aging, adipocytes are the major cell types that constitute the bulk of thymic microenvironment. Understanding the origin of thymic adipocytes and mechanisms responsible for age-related thymic adiposity is thus germane for the design of long lasting thymic rejuvenation strategies. We have recently identified that ghrelin, an orexigenic anti-inflammatory peptide, can partially reverse age-related thymic involution. Here we demonstrate that Ghrl and ghrelin receptor (growth hormone secretagogue receptor (GHSR)) are expressed in thymic stromal cells and that their expression declines with physiological aging. Genetic ablation of ghrelin and GHSR leads to loss of thymic epithelial cells (TEC) and an increase in adipogenic fibroblasts in the thymus, suggesting potential cellular transitions. Using FoxN1Cre;R26RstopLacZ double transgenic mice, we provide qualitative evidence that thymic epithelial cells can transition to mesenchymal cells that express proadipogenic regulators in the thymus. We found that loss of functional Ghrl-GHSR interactions facilitates EMT and induces thymic adipogenesis with age. In addition, the compromised thymic stromal microenvironment due to lack of Ghrl-GHSR interactions is associated with reduced number of naive T cells. These data suggest that Ghrl may be a novel regulator of EMT and preserves thymic stromal cell microenvironment by controlling age-related adipocyte development within the thymus.

The specialized three-dimensional thymic meshwork is composed of cortex and medulla, which is mainly comprised of distinct developing T cell subsets and diverse specialized thymic stromal cell populations (1). At birth, the thymocytes are the predominant cell types in the thymus; however, by the fifth decade of life in healthy humans, greater than 80% of thymic microenvironment is composed of lipid-laden adipocytes (2). The *raison d'être* of thymus is to produce naive T cells and

establish the T cell arm of immunity, whereas the function of adipocytes is to regulate energy homeostasis (3). Therefore, the development of adipocytes within a small lymphoid organ like the thymus is puzzling given its unlikely impact on overall energy homeostasis. Nonetheless, considering that the aged thymus is almost entirely replaced with adipocytes, the reconstitution strategies for thymic function in the elderly may be limited by the presence of terminally differentiated adipocytes in thymic space.

Given that the thymus lacks a pool of self-renewing lymphoid progenitors and needs to be continually seeded by hematopoietic stem cell from bone marrow (4), the replacement of thymic microenvironment with adipocytes could interfere with T cell generation. Furthermore, the homing of hematopoietic stem cell from bone marrow to thymus is orchestrated by a complex array of chemokines produced by TEC[2] at the cortico-medullary junction, the site of entry of progenitors into thymus (5). In addition, the cortical and medullary TECs provide a unique microenvironment and cell-cell contact and produce growth factors required for various aspects of T cell development (5). Thus, the success of hematopoietic stem cell-based experimental therapies for thymic restoration requires a functional thymic microenvironment. This is evident as the progenitor cells from the young animals develop into defective naive T cells when introduced in an aging thymic microenvironment (6, 7). The age-related reduction in thymopoiesis is due to multiple causes including the loss of TEC populations (8), defects in lymphoid progenitors (9, 10), and alteration in growth factors and hormones (11).

Ghrelin is a 28-amino-acid octanoylated peptide that is predominantly produced from the stomach in response to the negative energy balance (12). Apart from being a potent inducer of GH production, ghrelin is also the only known circulating orexigen (12). We and others have demonstrated that ghrelin exerts potent effects on immune cell subsets by inhibiting the

[2] The abbreviations used are: TEC, thymic epithelial cell; cTEC, cortical TEC; mTEC, medullary TEC; Ghrl, ghrelin; GH, growth hormone; GHSR, growth hormone secretagogue receptor; TSC, thymic stromal cells; EMT, epithelial-to-mesenchymal transition; PPAR, peroxisome proliferator-activated receptor; DAPI, 4′,6-diamidino-2-phenylindole; RT-PCR, real-time-PCR; EVA, early V antigen; AIRE, autoimmune regulator; IL, interleukin; PVS, perivascular space; PEPCK, phosphoenolpyruvate carboxykinase; MHCII, major histocompatibility complex II; FACS, fluorescence-activated cell sorter.

proinflammatory cytokines in a growth hormone secretagogue receptor (GHSR)-dependent mechanism (13, 14). Interestingly, ghrelin and GHSR are also expressed at lower levels in various organs and cell types including thymus (13, 15). The ghrelin supplementation in old mice increases thymopoiesis, whereas animals lacking ghrelin and GHSR have reduced thymic output with age (16). During the course of these studies, we observed that ghrelin infusions led to reduction of adipogenic lipid-expressing cells, whereas the absence of ghrelin signaling was associated with increased thymic adipocytes (16). This prompted us to investigate the mechanisms responsible for the generation of adipocytes in the thymus during aging.

The adipose tissue is believed to be of mesodermal origin; however, precise lineage of white and brown adipocytes remains to be determined (17), and the origin of thymic adipocytes is also unknown. One view is that adipocytes "infiltrate" the perivascular space of the thymus (18). However, evidence that large lipid-filled adipocytes can migrate and squeeze through tight intercellular spaces in thymic architecture is unavailable. Indeed, it has been speculated that adipogenic progenitors may undergo specific adipogenesis within the thymus and that the prevailing view of adipocyte trafficking in the thymus may be overly simplistic (3, 11). Based on the studies of fibroblast cell lines, it is known that differentiation of preadipocytes to adipocytes involves stages of growth arrest, clonal expansion, early differentiation, and terminal differentiation (19). It is also known that $\gamma 1$ and $\gamma 2$ isoforms of nuclear peroxisome proliferator-activated receptor (PPAR) generated as a result of alternative splicing and promoter usage are induced upon adipogenesis and are required for the maintenance of the differentiated state of the adipocyte (20). A preadipocyte expressing lipid and PPARγ is thus committed to an adipocyte fate; however, it is unknown whether a similar transcriptional program is initiated during ectopic adipocyte development in the thymus. In addition, cellular origin and mechanisms regulating adipogenic programming in the thymus remain to be ascertained.

In this report, we investigated a role for ghrelin-ghrelin receptor expression in TSC differentiation into adipogenic cells in the aging thymus. By genetically marking the TECs and fate-mapping experiments, we provide evidence that epithelial-to-mesenchymal transition (EMT) may be one potential source of adipocytes in the aging thymus. We found that disruption of ghrelin signaling accelerated EMT and increased thymic adiposity, which was correlated with reduced naive T cells.

EXPERIMENTAL PROCEDURES

Mice—The FoxN1-Cre mice were generated and bred to ROSA26RlacZ mice as described previously (21). The generation of Ghrl and GHSR mice has been described previously (22). A cohort of 12-month-old female C57/B6 mice ($n = 12$) mice and *ad libitum* fed ($n = 20$) mice was purchased from the NIA-aging rodent colony (Harlan Sprague-Dawley, Indianapolis, IN). All mice were maintained under pathogen-free conditions and fed normal chow diet. All protocols were approved by the Institutional Animal Care and Use Committee of Baylor College of Medicine, University of Georgia, and Pennington Biomedical Research Center.

Thymic Stromal Cell Culture—Thymic lobes were cleaned of fat and connective tissue, and the capsule was nicked with scissors. Then thymi were flush out as thymocytes in RPMI 1640. Thymi were then treated for 10 min at 37 °C with an enzymatic mixture containing 0.125% collagenase D (Roche Diagnostics), 0.1% DNase type I (Roche Diagnostics) in RPMI 1640. The supernatant was collected, and the digestion was repeated thrice. Thereafter, the thymic fragments were treated with 0.125% collagenase/Dispase (Roche Diagnostics), 0.1% DNase I in RPMI 1640. Cells were filtered through 100-μm mesh and spun at 13,000 rpm for 5 min. The CD45-positive cells were depleted using magnetic beads and CD45$^-$ cells were seeded in 24-well culture plates and cultured for 14 days in Dulbecco's modified Eagle's medium nutrient F12 (with 15 mM HEPES, NaHCO$_3$, L-glutamine, Invitrogen) supplemented with 3 μg/ml insulin, 20 ng/ml epidermal growth factor, 100 units/ml penicillin-streptomycin, and 10% fetal bovine serum. Cultures were maintained at 37 °C and 5% CO$_2$, and the medium was changed twice a week. On day 14, cells were induced to differentiate by changing the medium to Dulbecco's modified Eagle's medium/F12 containing 10% fetal bovine serum, 0.5 mM 3-isobutylmethylxanthine, 1 μM dexamethasone, and 1.7 μM insulin (MDI). After 48 h, the cells were collected to extract total RNA.

Cell Preparations and FACS Analysis—The thymi were enzymatically digested as described (23). The following monoclonal antibodies were directly coupled to phycoerythrin, fluorescein isothiocyanate, allophycocynanin, or phycoerythrin-CyT and commercially purchased from eBiosciences: CD3, MHCII, Ly5.1, CD45, CD44, CD62L, CD4, and CD8. The CD45 cells were gated out, and lipid-containing cells were analyzed using LipidTox-fluorescein isothiocyanate (Invitrogen). The FACS-Calibur was used for analysis, and all data were analyzed by post-collection compensation using the FlowJO (Tree Star Inc.) software.

Immunohistochemistry—The thymi obtained from mice were flash-frozen and subsequently embedded in Stephens Scientific frozen section medium (Riverdale, NJ) and cut into 5–10-μm-thick cryostat sections. At least three serial sections were utilized for each staining. Tissue sections were then fixed with 4% buffered paraformaldehyde and stained with various combinations of the following primary antibodies to mouse antigens: unconjugated rat antibody to ERTR7 (HM1086, Cell Sciences); unconjugated mouse monoclonal antibody to PPARγ (E-8, Santa Cruz); unconjugated rabbit polyclonal anti-aP2 (2120S, Cell signaling); unconjugated rat monoclonal antibody to TROMA-1 (Developmental Studies Hybridoma Bank (DSHB), University of Iowa); biotin-conjugated mouse monoclonal antibody to UEA-1 (Vector Laboratories); unconjugated rabbit antibody to FSP1 (ab27957, AbCam), CD31 (12-0311-82, eBiosciences); or unconjugated mouse antibody to β-galactosidase (Z378B, Promega). Slides were incubated with the following secondary regents: Alexa Fluor 488- or Alexa Fluor 594-conjugated polyclonal chicken anti-mouse IgG; Alexa Fluor 488-conjugated polyclonal donkey anti-rat IgG; Alexa Fluor 488- or Alexa Fluor 594-conjugated polyclonal chicken anti-rabbit IgG; of Alexa Fluor 594-conjugated streptavidin (Molec-

TABLE 1

Sequences of conventional RT-PCR primer pairs

Gene	Forward 5′ → 3′	Reverse 5′ → 3′
18S	Universal 18S internal standard	
Ghrl	GGCATTCCAGGTCATCTGTC	GCCTGTCCGTGGTTACTTGT
GHSR	CTCCTCAGGGGACCAGATTT	CTTCCTCCCGATGAGACTGT

TABLE 2

Sequences of real-time PCR primer pairs

Gene	Forward 5′ → 3′	Reverse (5′ → 3′)
18S	GTCTGTGATGCCCTTAGATG	AGCTTATGACCCGCACTTAC
Ghrl	CTGAGCTCCTGACAGCTTGA	ACCCAGAGGACAGAGGACAA
GHSR	GGAAAACAGATATCTTCCCACG	GGGACCAGAACCACAAACAG
EVA	GGCTGGCTTTCCCTGATGTAT	TTAACCGAACATCTGTCCCGT
Aire	GGTTCTGTTGGACTCTGCCCTG	TGTGCCACGACGGAGGTGAG
IL-7	GGGAGTGATTATGGGTGGTGAG	TGCGGGAGGTGGGTGTAG
KGF	TTGACAAACGAGGCAAAGTG	CCCTTTGATTGCCACAATTC
FSP1	CAGCACTTCCTCTCTCTTGG	TTTGTGGAAGGTGGACACAA
E-cadherin	GAGGTCTACACCTTCCCGGT	AAAAGAAGGCTGTCCTTGGC
Foxc2	ACAGTTGGGCAAGACGAAAC	AGTGCGGATTTGTAACCAGG
N-cadherin	AAGGACAGCCCCTTCTCAAT	CGTCCACCTTGAAATCTGT
PPARy2	GCCTATGAGCACTTCACAAGAATT	TGCGAGTGGTCTTCCATCAC
aP2	GCGTGGAATTCGATGAAATCA	CCCGCCATCTAGGGTTATGA
Perilipin	GACACCACCTGCATGGCT	TGAAGCAGGGCCACTCTC
PGAR	GGAAAAGTCCACTGTGCCTC	AAGATGACCCAGCTCATTGG
CD36	CCTGCAAATGTCAGAGGAAA	GCGACATGATTAATGGCACA
PEPCK	AACTGTTGGCTGGCTCTC	GAACCTGGCGTTGAATGC

ular Probes). Nuclei were visualized with 4′,6-diamidine-2′phenylindole dihydrochloride (DAPI, Sigma). Negative controls as obtained by occulting the primary antibody or by using an unrelated IgG displayed no specific labeling. Fluorescence mounting solution (Vector Laboratories) was applied to slides and observed with a Zeiss Axioplan 2 and Zeiss confocal microscope. In addition, for the visualization of lipid droplet, frozen thymic sections were fixed with 4% buffered paraformaldehyde and then stained with LipidTox-Green (Invitrogen) for 20 min. Images were captured using laser scanning confocal microscope (LSM 510, Carl Zeiss Inc).

Real-time RT-PCR—Total RNA was prepared with RNAzol (Isotex Diagnostics). The samples were DNase digested to remove any potential genomic DNA contamination, and the cDNA synthesis and real-time RT-PCR were performed as described previously (13, 16). Real-time RT-PCR analyses were done in duplicate on the ABI PRISM 7900 sequence detector TaqMan system with the SYBR Green PCR kit as instructed by the manufacturer (Applied Biosystems). The primer pairs used for RT-PCR are shown in Tables 1 and 2.

Statistical Analysis—The results are expressed as the mean ± S.E. The differences between means and the effects of treatments were determined by one-way analysis of variance using Tukey's test, which protects the significance ($p < 0.05$) of all pair combinations.

RESULTS

Ghrelin and GHSR Expression in Thymic Stromal Cells—When compared with stomach and central nervous system, the Ghrl and GHSR are expressed at lower levels in T cells (13). The GHSR expression has been found to be partially co-localized with keratin 5 expressing mTECs and on keratin 8 cTECs (16). These findings led us to investigate specific Ghrl and GHSR expression in purified TSC from young and aging mice. Both Ghrl and GHSR mRNA were expressed in CD45$^+$ lymphoid as well as CD45$^-$ TSC (Fig. 1A). Interestingly, when com-
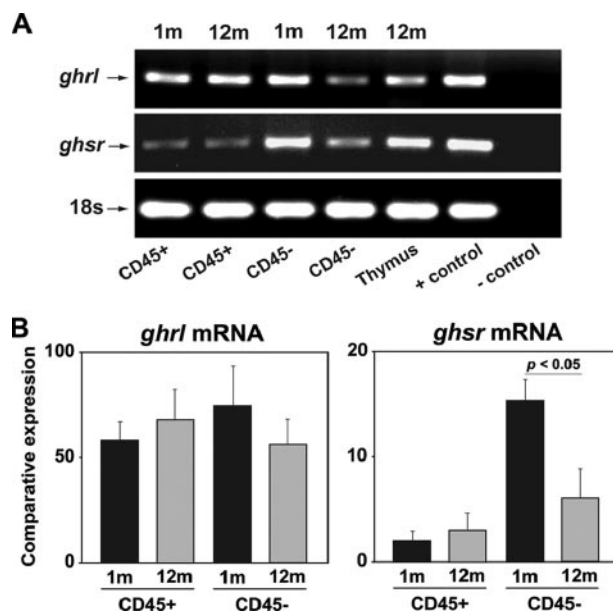

FIGURE 1. **Ghrelin and GHSR expression in thymic stromal cells.** *A*, the RT-PCR analysis of Ghrl and GHSR mRNA in cells isolated from 1- and 12-month-old thymi. A total of six thymi each from these age groups were pooled to isolate the cells and experiment was repeated thrice. *B*, real-time PCR analysis and quantitation of Ghrl and GHSR expression in CD45+ and CD45− cells in thymi of 1- and 12-month-old mice. Data are expressed as mean ± S.E.

pared with 1-month-old mice, we detected a significant reduction of GHSR mRNA expression in CD45$^-$ TSC fraction of 12-month-old animals, whereas no significant ($p < 0.05$) change in Ghrl could be observed (Fig. 1B).

Loss of Ghrelin Signals Compromises Thymic Stromal Cell Microenvironment—Aging is known to severely impact the integrity of the TEC compartment (8, 23). The growth factors required for maintenance of TECs in the aging thymic microenvironment are incompletely understood. Ghrelin regulates T cell function via a GHSR-dependent mechanism (13, 16), and available evidence indicates that GHSR is also required for the anabolic effects of ghrelin (22). To assess the impact of deficient ghrelin-mediated signals, we investigated the 10–15-month-old GHSR$^{-/-}$ mice. When compared with 10-month-old age-matched wild type mice, the GHSR$^{-/-}$ animals displayed loss of keratin 8$^+$ cTEC and UEA1$^+$ mTEC cells in the thymus (Fig. 2A). We then investigated a separate cohort of mice (12 months old from Baylor College of Medicine animal facility) and demonstrate that similar to our IHC results, this cohort of GHSR$^{-/-}$ mice also had a reduced number of CD45$^-$MHCII$^+$Ly51$^-$ mTEC and CD45$^-$MHCII$^+$Ly51$^+$ cTEC cells (Fig. 2B). We next studied the expression of stromal genes that play a key role in thymic function. The early V antigen (*EVA*) is a constitutively cTEC expressed gene (24), and autoimmune regulator (*Aire*), expressed in a subset of mTEC cells (25), is critical for thymic function. We observed that 12-month-old Ghrl$^{-/-}$ and GHSR$^{-/-}$ mice had significant reduction in *EVA, Aire,* and *IL-7* mRNA expression with no change in fibroblast growth factor-7 (*FGF7*) levels (Fig. 2C). These findings are consistent with our hypothesis that ghrelin signaling may be required for TEC maintenance.
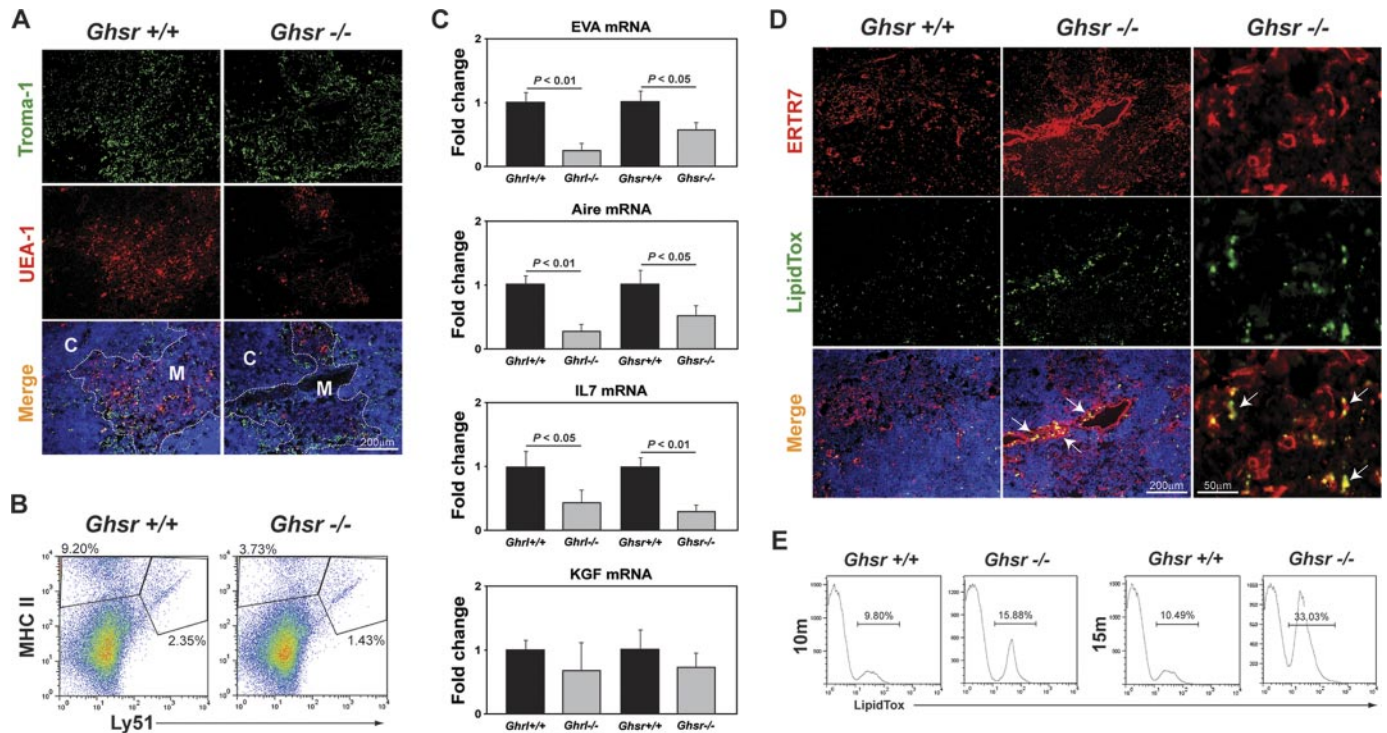
FIGURE 2. **Loss of ghrelin signals compromises thymic stromal microenvironment during aging.** *A*, the thymic cryosections were labeled for keratin 8$^+$ cortical TEC using anti-TROMA1 antibody, and medullary TECs were identified by biotin-conjugated plant lectin *Ulex europaeus agglutinin* 1 (UEA-1). Nuclei were counterstained with DAPI. *C*, cTEC; *M*, mTEC. *B*, the CD45$^-$ thymic stromal cells were stained for Ly51 and MHCII to distinguish cTEC and mTEC cells. A deletion of GHSR reduces both cTEC and mTEC population in 12-month-old mice. *C*, the real-time-PCR analysis of EVA, Aire, IL-7, and keratinocyte growth factor (*KGF*) in thymi of 12-month-old GHSR and Ghrl null mice and control littermates. *D*, the thymic cryosections were labeled for the fibroblast-specific marker ERTR7 (*red*) and LipidTox (*green*). Nuclei were counterstained with DAPI. The *arrows* indicate the lipid-expressing fibroblasts in the PVS of thymus. A representative image from a minimum of four thymi in each group is shown. *E*, the CD45$^-$ TSC were pooled from six thymi of control and GHSR null mice in 10-month-old and 15-month-old age groups and stained with LipidTox-fluorescein isothiocyanate, and FACS analysis was performed in two separate cohorts of mice.

Given our previous findings that 24-month-old GHSR$^{-/-}$ mice have increased adipocytes in thymic space (16), we next investigated whether thymic fibroblasts serve as adipogenic precursors during aging. Using ERTR7 as a marker of fibroblasts, we detected increased labeling for ERTR7 in 12-month-old GHSR$^{-/-}$ mice (Fig. 2*D*), whereas the isotype control antibody showed no specific staining (data not shown). Recent studies by Boyd and colleagues (26) have also demonstrated that aging is associated with increase in thymic fibroblasts. Interestingly, we observed an increase in lipid-expressing perivascular fibroblasts in GHSR$^{-/-}$ mice, suggesting their adipogenic nature. We next quantitated the lipid-expressing cells in the thymus during aging using FACS analysis and demonstrated that in 10- and 15-month-old mice, the absence of ghrelin-mediated signals leads to significant increase in CD45$^-$LipidTox$^+$ adipogenic cells in the thymus (Fig. 2*E*). Thus, our data suggest that GHSR may serve to limit the adipogenesis within TSCs and that loss of GHSR-mediated signals may contribute to increased thymic adipogenic cells.

Deficient Ghrelin Receptor Signaling Regulates EMT in Aging Thymus—Considering that GHSR null animals exhibited reduction in TECs, an increase in thymic fibroblasts led us to hypothesize that this might be related to the process of EMT. The EMT is a process whereby epithelial cells assume a mesenchymal phenotype via cellular transition (27). The EMT is a defining structural mechanism of organ development during embryogenesis (27). However, in adult life, the EMT can also be

a source of local tissue fibroblasts, which are known to cause several fibrotic diseases (28). An important question arising from the findings of age-related loss of thymic epithelial cells and increase in fibroblast is whether EMT is an underlying mechanism in the aging thymus. Also, mesenchymal cells are highly plastic and multipotent in nature and can give rise to adipocytes *in vitro* (29). However, the determination of cell lineage by gene expression analysis or *in vitro* studies is insufficient because transcriptional signatures are transient and subject to epigenetic or regulatory influences. Hence, the true origin of a cell can only be determined by genetic lineage tracing. To this end, we developed the *FoxN1Cre;R26RstopLacZ* double transgenic mouse to test the hypothesis that EMT contributes toward generation of a subset of local thymic fibroblasts.

The *FoxN1* gene is expressed by the TECs, and in *FoxN1Cre* mice, the IRES-Cre cassette has been knocked-in into the 3′-untranslated region of FoxN1 genomic locus; thus, Cre expression causes a permanent genetic change in all cells that express FoxN1 (21). In the *R26RstopLacZ* indicator mice, the *lacZ* gene is expressed upon Cre-mediated excision of a loxP STOP cassette. Therefore, in the *FoxN1Cre;R26RstopLacZ* double transgenic mice, the lacZ expression persists in cells that have ever expressed FoxN1, despite any subsequent age-related phenotypic alterations or cellular transitions (Fig. 3*A*).

Studies from Eric Nielson and colleagues (30) have identified fibroblast-specific protein-1 (*FSP1*) as a marker of cells under-
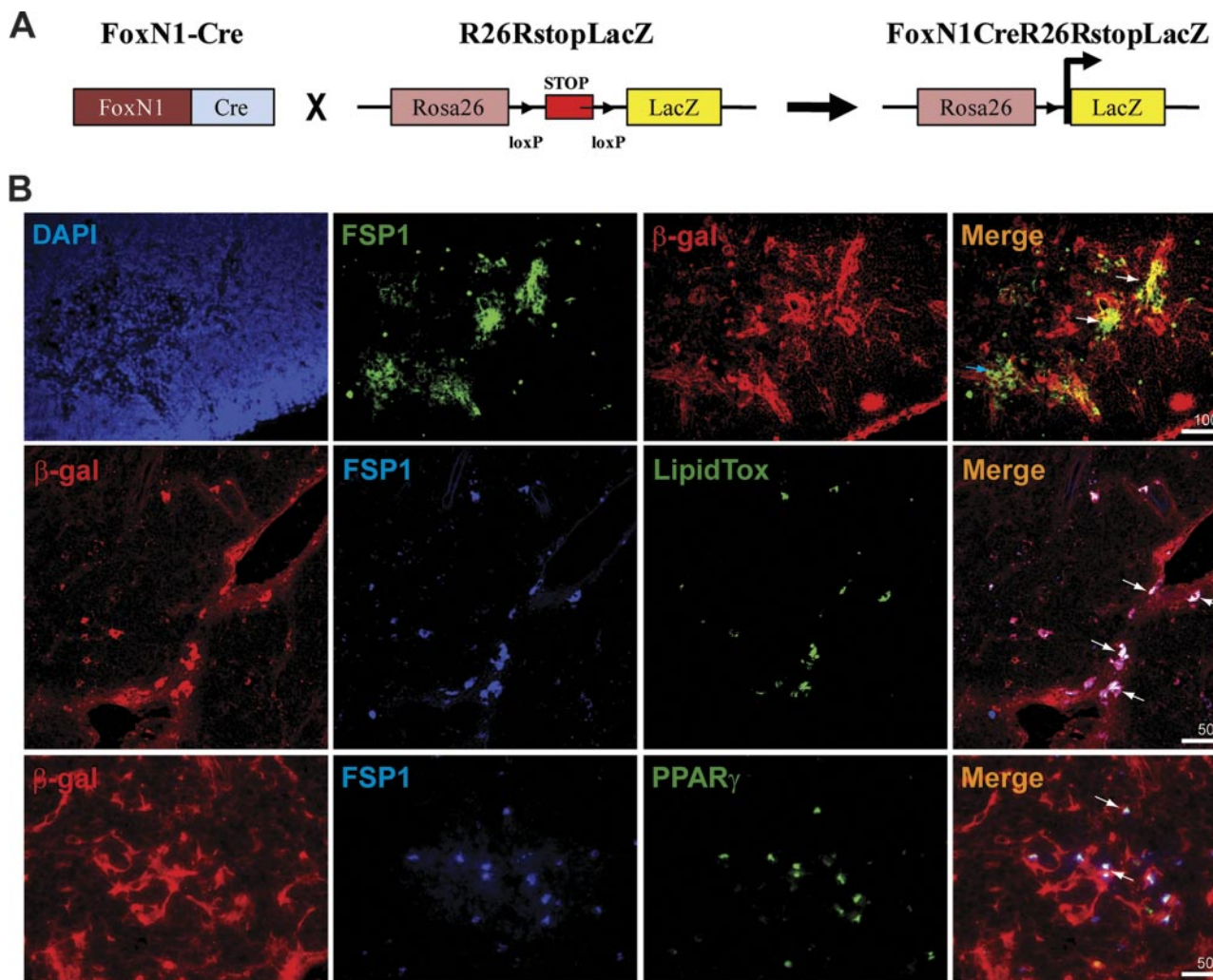
FIGURE 3. **Ghrelin regulates epithelial-to mesenchymal transition in the thymus.** *A*, the FoxN1-Cre-expressing mice were bred with indicator mice that contain the *LacZ* gene integrated into the ubiquitous ROSA26 locus downstream of a floxed transcriptional STOP sequence. Expression of Cre recombinase in TECs excised the floxed STOP sequence and indelibly marked the cells with LacZ. *B*, immunofluorescence triple labeling in 3-month-old *FoxN1Cre; ROSA26RstoplacZ* reporter mice thymus with DAPI (*blue*), antibodies to β-galactosidase (indelibly marked TEC), and FSP-1 (EMT marker). The EMT is evident by medullary expression and co-localization of FSP1 with β-galactosidase. Thymic cryosections of 3-month-old *FoxN1Cre;ROSA26RstoplacZ* mice were triple labeled with antibodies to FSP1 (*blue*), β-galactosidase (*red*), and neutral lipid by LipidTox (*green*) or PPARγ (*green*). A representative image ($n = 4$) shows lipid expression within a β-galactosidase and FSP1 co-expressing cells in the thymic PVS.

going EMT. The *FSP1* gene contains a position and promoter-dependent proximal element between -187 and -88 bp called fibroblast transcription site-1 (FTS-1), which is active in fibroblast but not in epithelium (28, 30). Thus, the first 2500 bp of upstream promoter and first intron in FSP1 gene provide all the critical instructions for selective FSP1 expression in fibroblast. Importantly, during embryonic development, the FSP1 expression in fibroblast is detected between embryonic days 9 and 12, which is relatively late in somatogenesis (27). FSP1 is not expressed in primary mesenchymal cells and is present in fibroblast cells derived from secondary epithelium (28, 30) and is therefore a strong indicator of EMT. In the thymi of *FoxN1Cre; R26RstopLacZ* mice, LacZ (indelibly marked for thymic epithelial cells) co-localizes with FSP1 (Fig. 3*B*), suggesting EMT. Interestingly, the majority of FSP1 expression was co-localized with the medullary FoxN1-expressing cells. However, not all FSP1^{+} cells expressed LacZ, and hence, a subset of these local fibroblasts is not of epithelial origin and may be derived from as of yet unknown cellular lineages.

Although our findings suggest that thymic fibroblast may serve as an adipogenic precursor in the aging thymus, the exact provenance of thymic adipocytes is unknown. It has recently been shown that cells generated as a result of EMT have stem-like properties (29) and that mesenchymal cells can readily differentiate into adipocytes, chondrocytes, and osteocytes (17). Interestingly, almost four decades ago, Friedenstein (31) in his pioneering work showed that "transitional epithelial cells" in the thymus are amenable to osteogenesis *in vitro*. Together with our initial observations that adipogenetic fibroblasts increase with age and Friedenstein's seminal findings (31), we hypothesized that EMT may be one potential source of multi-potent cells and that the EMT-derived cells serve as adipogenic progenitor in aged thymus.

The adipogenic cells in murine thymus can be detected in various regions, including perivascular space, septae, cortex, medulla, and subcapsular regions. It has previously been hypothesized that adipocytes infiltrate in the perivascular space (PVS) of the thymus (2, 18). Interestingly, in 3-month-old
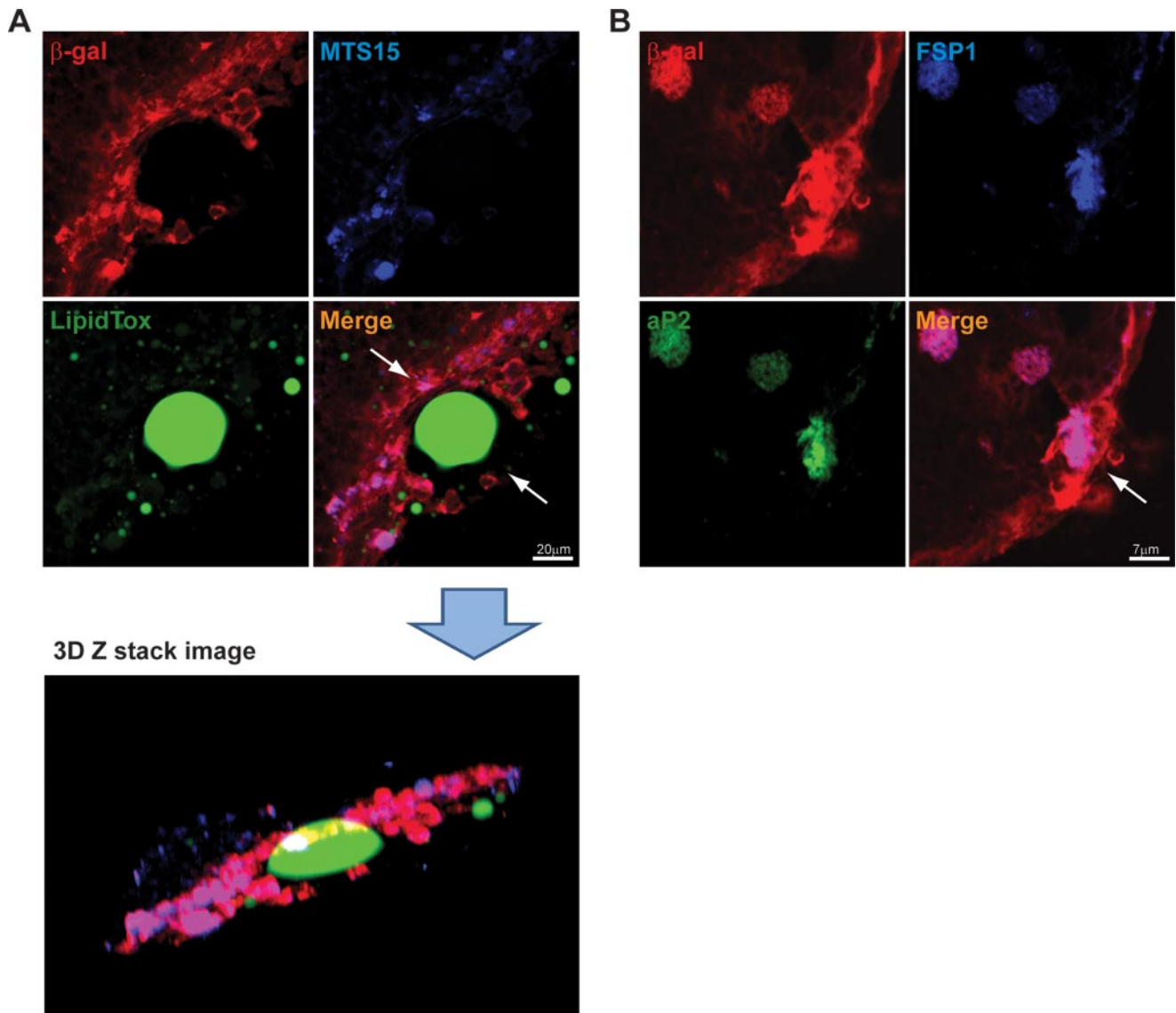
FIGURE 4. **Co-localization of MTS15, FSP1, aP2, and LipidTox in thymus of *FoxN1Cre;ROSA26RstoplacZ* mice.** *A*, thymic cryosections of 6-month-old *FoxN1Cre; ROSA26RstoplacZ* labeled with MTS15 (*fibroblast marker*), β-galactosidase (*red*), and LipidTox (*green*). The confocal Z-stack image reconstruction in three-dimensional (*3D*) orientation depicts the presence of LipidTox-stained cells within the thymic subcapsule. The merge of β-galactosidase (*red*) and MTS15 (*blue*) appears as cyan cells enveloping the large unilocular lipid vacuole. *B*, the subcapsular region of thymus showing co-localization of β-galactosidase (*red*), FSP1 (*blue*), and aP2 (*green*).

FoxN1Cre;R26RstopLacZ mice, small lipid droplet-expressing cells co-localized with β-galactosidase- and FSP1-expressing cells in the PVS of the thymus (Fig. 3*B*, *middle panel*). The β-galactosidase expression in PVS of *FoxN1Cre;R26RstopLacZ* mice is consistent with recent studies showing Ker5 TEC localization around thymic blood vessels (32) and the spatial relationship of mTECs with thymic vasculature (33). Given that recombination at the rosa26 locus induced by Cre recombinase driven by FoxN1 is heritable and irreversible, the cells with "TEC footprints" can be traced despite any age-related alterations in FoxN1 epithelial cells. Considering that nuclear receptor PPARγ is required for an adipocyte phenotype (19, 20), we further demonstrate that EMT cells also express PPARγ and are hence adipogenic (Fig. 3*B*, *lower panel*). Collectively, our findings suggest that EMT may be one potential source of adipogenic cells and that these cells arise in the thymus via cellular transition mechanisms and not by "infiltration."

Apart from PVS, thymic adipocytes are also present in other regions of murine thymus. Therefore, we further examined 6-month-old *FoxN1Cre;R26RstopLacZ* mice to understand whether EMT contributes to adipocyte development. We observed that by 6 months of age, larger lipid-containing cells were readily detected within the FoxN1-expressing cells in the thymic subcapsular region. The triple color confocal analysis revealed that large lipid vacuole-containing adipocytes are lined by MTS15 and FoxN1-LacZ tagged cells (Fig. 4*A*). The Z-stack confocal image reconstruction revealed that lipid-expressing cells are present within the subcapsular region (Fig. 4*A*). Thus, the origin of subcapsular adipocyte development with age may be due to EMT and may not be due to infiltration or "invasion" of perithymic adipocytes through the thymic capsule. We further investigated subcapsular adipocytes using fatty acid binding-protein-4 or aP2, a terminal marker of adipogenic
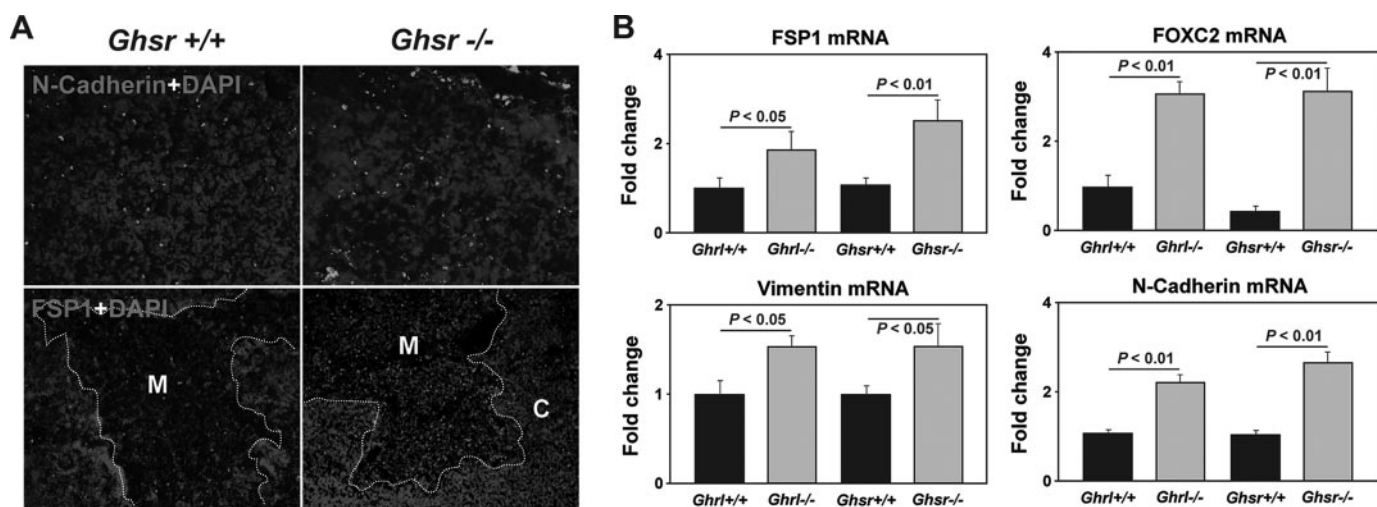
FIGURE 5. **Loss of Ghrel in signaling activates EMT inducers in the thymus.** *A*, the 10-month-old control and GHSR knock-out mice thymi were stained for N-cadherin (*green*) and FSP-1 (*red*). Nuclei were counterstained with DAPI (*blue*). *B*, real-time-PCR analysis of EMT genes, *FSP1*, *vimentin*, *N-cadherin*, and *FOXC2* in the thymus. Data are expressed as mean ± S.E. with 6–8 mice per group.
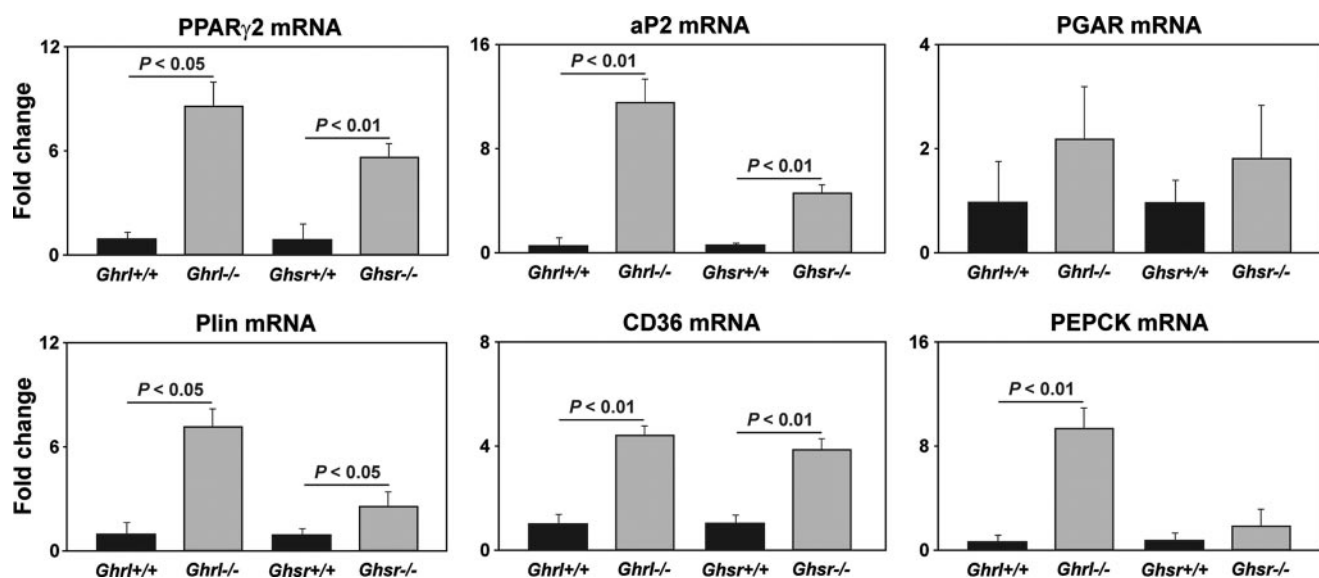

FIGURE 6. **Deficient ghrelin signaling induces adipogenic programming in the thymus.** Real-time-PCR analysis of adipogenesis regulating transcripts in the thymus of 12-month-old Ghrl- and GHSR-deficient and age-matched control mice is shown. Data are expressed as mean ± S.E. with 6–8 mice in each group. *PGAR*, PPAR-γ angiopoietin-related.

cells (19, 20). Consistent with our hypothesis, we found that aP2 is expressed in FSP1$^+$β-galactosidase$^+$ cells within the thymic subcapsule, suggesting that EMT can give rise to terminal adipogenic cells within the thymus (Fig. 4). These findings suggest that TECs undergo EMT and that FSP1$^+$ mesenchymal cells may be one source of thymic adipocytes.

We next investigated the mechanisms responsible for the emergence of adipogenic EMT cells in the aging thymus. We observed increased localization of N-cadherin and FSP1 in the GHSR$^{-/-}$ mice (Fig. 5*A*). We next quantified the EMT transcripts in Ghrl$^{-/-}$ and GHSR$^{-/-}$ mice and found that deficient ghrelin signaling led to a significant increased expression of EMT transcripts, FSP1, FOXC2, Vimentin, and N-cadherin (30) in the thymus (Fig. 5*B*). Thus, our findings suggest that ghrelin may maintain the thymic stromal microenvironment by inhibiting EMT and preserves TEC integrity. This is consistent with our previous findings that ghrelin infusion in

14-month-old mice can restore the age-related loss of TECs (16).

Accelerated Adipogenic Programming Due to Dysfunctional Ghrelin-GHSR Axis in Aging Is Associated with Reduced Naive T Cells—The cells arising due to EMT are multipotent in nature (29). Given our findings of increased EMT in Ghrl$^{-/-}$ and GHSR$^{-/-}$ mice and higher expression of lipid-expressing thymic fibroblasts, we hypothesized that specific proadipogenic regulators may be responsible for thymoadipogenesis. It has been demonstrated that nuclear receptor PPARγ2 is necessary and sufficient for adipogenesis and that *PEPCK* is considered as a downstream gene indicative of PPARγ activity (19, 20). The aP2 is a key regulator of adipogenesis, whereas the presence of perilipin that coats the lipid droplets and scavenger receptor CD36 is required for lipid processing and packaging (19, 20). Consistent with our hypothesis of specific adipogenic programming in the aging thymus, we detected intact adipogenic tran-
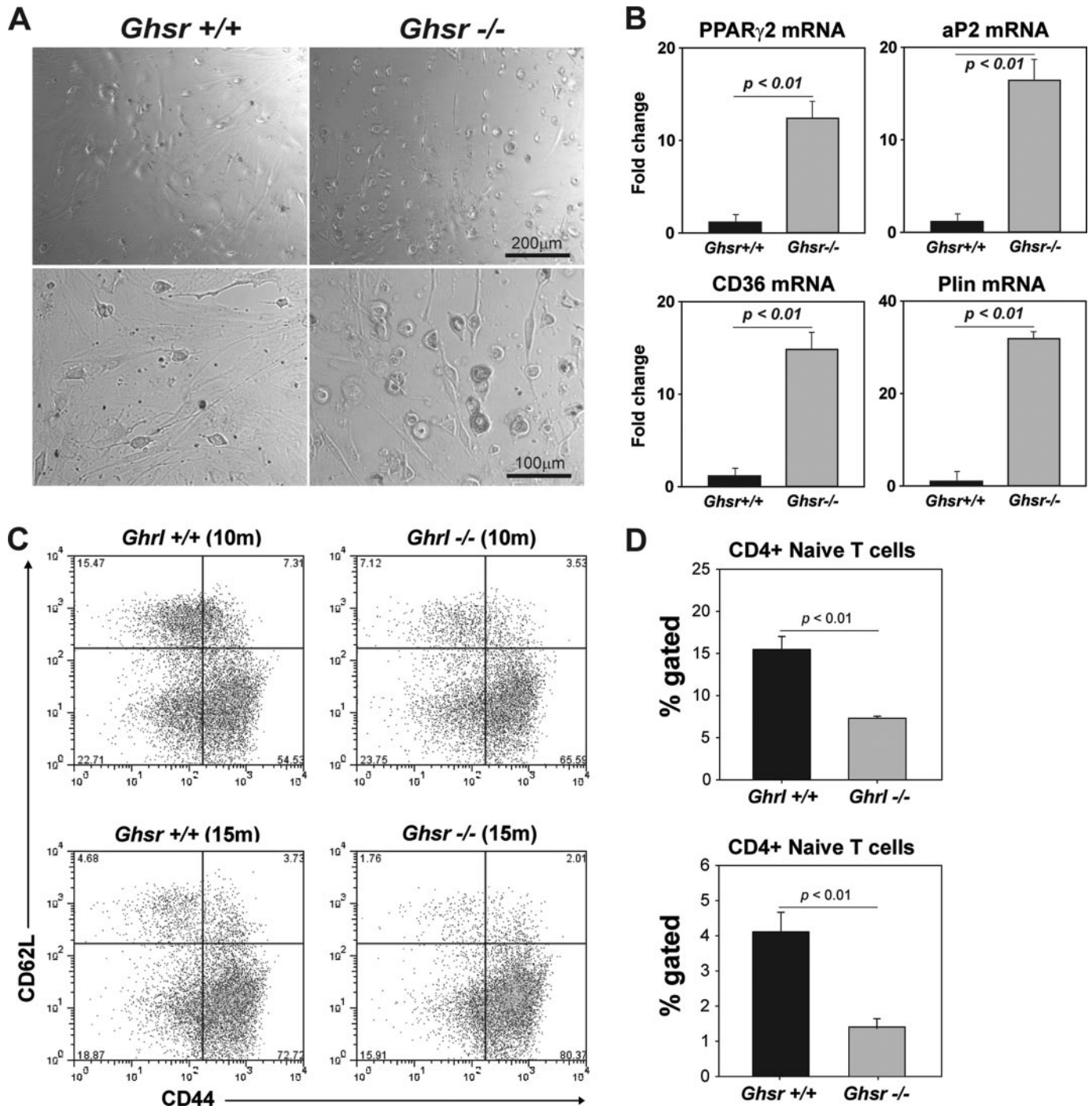
FIGURE 7. **Deficient ghrelin-mediated signaling induces adipogenesis in thymic stromal cells.** *A*, the CD45− TSC from control and GHSR$^{-/-}$ mice (10 months old) and cultured *in vitro* and treated with adipogenesis inducing mixture containing 0.5 mM 3-isobutylmethylxanthine (*M*), 1 μM dexamethasone (*D*), and 1.7 μM insulin (*I*). 48 h after MDI treatment, adipogenesis was evident by higher lipid accumulation and rounding of GHSR$^{-/-}$ TSCs. *B*, real-time-PCR analysis of proadipogenic transcripts in TSC exposed to MDI treatment. Data are expressed as mean ± S.E. and repeated thrice in triplicate wells. *C*, the FACS analysis of naive and effecter/memory CD4 and CD8 cells in spleen of 10-month-old Ghrl and 15-month-old GHSR null mice with control litter mates. *D*, deletion of Ghrl and GHSR significantly (*p* < 0.05) reduces the naive (CD62L$^+$CD44$^-$) cells in spleen.

scriptional machinery in aging thymi. Interestingly, loss of Ghrl-GHSR signals led to a markedly increased expression of PPARγ2, aP2, perilipin, and CD36 (Fig. 6). We also observed elevated expression of PEPCK, which is indicative of elevated PPARγ2 activity, whereas no change in expression of PPARγ-ligand induced target gene *PGAR* (for PPAR-γ angiopoietin-related) was observed.

These data prompted us to next investigate whether the TSCs of GHSR$^{-/-}$ animals display cell-intrinsic adipogenic programming. We purified the TSCs and cultured them *ex vivo* to track their development into adipocytes. Considering that TSCs express Ghrl and GHSR, we hypothesized that GHSR-mediated signals (via autocrine Ghrl source) are required for adipogenesis. We found that when TSCs were exposed to an

adipogenic mixture containing methylisobutylxanthine, insulin, and dexamethasone, the TSC from GHSR$^{-/-}$ mice developed into adipocytes at an accelerated rate (Fig. 7*A*). Consistent with our hypothesis that TSC-derived ghrelin serves to limit thymoadipogenesis, we found that GHSR-deficient TSCs in culture expressed significantly higher levels of PPARγ2, aP2, perilipin, and CD36 (Fig. 7*B*). These data suggest that ghrelin expression in TSC may be physiologically relevant and serves as "adipogenic brake" because in the absence of viable GHSR signaling (despite autocrine ghrelin), TSC cells develop into adipocytes. We also found that increased thymoadipogenesis led to reduced numbers of naive CD4 cells in Ghrl and GHSR null mice (Fig. 5*C*), suggesting that increased thymic adiposity correlates with reduced thymic output.

DISCUSSION

The aging-induced defects in the structural elements and environment of the thymus are believed to play critical roles in reduced generation of recent thymic emigrants (3). One of the most dramatic changes in thymic environment with aging is a progressive increase in adipocytes in the thymic perivascular space, parenchyma, septa, cortex, and medulla with loss of epithelial and T lymphopoietic thymic zones into adipose tissue (2, 3). Thymic aging process is puzzling as it precedes that of most bodily tissues by a large margin. Also, loss of thymic function with increasing age is related to almost complete replacement of its microenvironment with adipose tissue. Despite overwhelming evidence in favor of this phenomenon, the mechanistic studies to define the origin and mechanism of adipocytes to thymic biology remain to be performed.

We have recently demonstrated that ghrelin can partially reverse age-related thymic involution (16). Interestingly, we observed that ghrelin supplementation in old mice reduced the lipid-expressing "preadipocyte-like" cell in the thymic parenchyma, whereas ghrelin knock-out mice had accelerated thymic involution with an increase in the number of thymic adipocytes (16). In addition, ghrelin infusions in aging mice led to an increase in thymic epithelial cells. Here, we demonstrate that ghrelin and GHSR are expressed in the TSC and that their expression declines in middle-aged mice. Consistent with our hypothesis that ghrelin-GHSR interactions may be required for maintenance of the thymic stromal microenvironment, we detected loss of TEC and increase in adipogenic fibroblasts in GHSR null mice. We have previously demonstrated that 24-month-old GHSR mice have increased adipocytes in thymic space and have reduced thymocyte numbers (16). It is well established that thymocytes are required for the maintenance of TEC (34). Thus, it is possible that loss of thymocytes in ghrelin and GHSR knock-out mice results in stromal cell alterations. Our findings suggest that certain thymic adipocytes originate from thymic stroma via a highly regulated process. Interestingly, IL-2 receptor γ chain mutant mice, which lack thymocytes and have severely atrophied thymi, do not show a default increase in adipocytes in the thymus (35). In addition, the young RAG$^{-/-}$ and severe combined immunodeficiency (SCID) mouse models, where thymus is severely involuted with reduced thymocyte cellularity, also lack adipocytes in the thymus (data not shown). Thus, adipocyte development in the thymus may be due to aging-specific cellular transition mechanisms. Using genetic fate-mapping experiments, we provide the first clear evidence that epithelial cell in the thymus transition into mesenchymal cells, which can be subsequently driven into adipocyte lineage during aging.

Interestingly, the loss of TEC and increase in adipogenic fibroblasts in GHSR null mice was coupled with an increase in EMT inducers in the thymus. Cells generated by EMT are multipotent (29); however, when generated in an aging thymic microenvironment, they appear to be restricted toward an adipocyte fate and not osteogenic, chondrogenic, or myogenic lineages. Considering that PPARγ is necessary and sufficient for committing a fibroblast to an adipogenic lineage, we investigated the expression of this transcription factor along with other key adipogenic regulators in the thymus. Consistent with our hypothesis that an increase in adipogenic genes may drive EMT cells into adipogenesis, we found that the absence of ghrelin-GHSR signals led to elevated adipogenic programming. Furthermore, purified TSCs of GHSR knock-out mice express high levels of adipogenic genes and show accelerated adipocyte development *ex vivo*. Given that with physiological aging, the TSCs lose GHSR expression and that GHSR$^{-/-}$ TSC develop into adipocytes suggests that ghrelin may be required for maintenance of TEC phenotype and retards adipogenic programming in the thymus. Collectively, our data provide evidence of a unique role of ghrelin in regulating age-related EMT and thymic adipogenesis, suggesting that ghrelin mimetic-based therapy may restore thymic function.

REFERENCES

1. Rodewald, H. R. (2008) *Annu. Rev. Immunol.* **26,** 355–388
2. Steinmann, G. G. (1986) *Curr. Top. Pathol.* **75,** 43–88
3. Dixit, V. D. (2008) *J. Leukoc. Biol.* **84,** 882–892
4. Bhandoola, A., von Boehmer, H., Petrie, H. T., and Zuniga-Pflucker, J. C. (2007) *Immunity* **26,** 678–689
5. Petrie, H. T., and Zuniga-Pflucker, J. C. (2007) *Annu. Rev. Immunol.* **25,** 649–679
6. Clise-Dwyer, K., Huston, G. E., Buck, A. L., Duso, D. K., and Swain, S. L. (2007) *J. Immunol.* **178,** 1321–1331
7. Mackall, C. L., Punt, J. A., Morgan, P., Farr, A. G., and Gress, R. E. (1998) *Eur. J. Immunol.* **28,** 1886–1893
8. Gui, J., Zhu, X., Dohkan, J., Cheng, L., Barnes, P. F., and Su, D. M. (2007) *Int. Immunol.* **19,** 1201–1211
9. Min, H., Montecino-Rodriguez, E., and Dorshkind, K. (2004) *J. Immunol.* **173,** 245–250
10. Zediak, V. P., Maillard, I., and Bhandoola, A. (2007) *Blood* **110,** 1161–1167
11. Taub, D. D., and Longo, D. L. (2005) *Immunol. Rev.* **205,** 72–93
12. Kojima, M., and Kangawa, K. (2005) *Physiol. Rev.* **85,** 495–522

13. Dixit, V. D., Schaffer, E. M., Pyle, R. S., Collins, G. D., Sakthivel, S. K., Palaniappan, R., Lillard, J. W., Jr., and Taub, D. D. (2004) *J. Clin. Investig.* **114,** 57–66

14. Gonzalez-Rey, E., Chorny, A., and Delgado, M. (2006) *Gastroenterology* **130,** 1707–1720

15. Gnanapavan, S., Kola, B., Bustin, S. A., Morris, D. G., McGee, P., Fairclough, P., Bhattacharya, S., Carpenter, R., Grossman, A. B., and Korbonits, M. (2002) *J. Clin. Endocrinol. Metab.* **87,** 2988–2991

16. Dixit, V. D., Yang, H., Sun, Y., Weeraratna, A. T., Youm, Y. H., Smith, R. G., and Taub, D. D. (2007) *J. Clin. Investig.* **117,** 2778–2790

17. Gesta, S., Tseng, Y. H., and Kahn, C. R. (2007) *Cell* **131,** 242–256

18. Hale, L. P., Clark, A. G., Li, J., Greer, P. K., and Byers Kraus, V. (2001) *Dev. Comp. Immunol.* **25,** 509–518

19. Farmer, S. R. (2006) *Cell Metab.* **4,** 263–273

20. Rosen, E. D., and Spiegelman, B. M. (2006) *Nature* **444,** 847–853

21. Gordon, J., Xiao, S., Hughes, B., III, Su, D. M., Navarre, S. P., Condie, B. G., and Manley, N. R. (2007) *BMC Dev. Biol.* **7,** 69

22. Sun, Y., Wang, P., Zheng, H., and Smith, R. G. (2004) *Proc. Natl. Acad. Sci. U. S. A.* **101,** 4679–4684

23. Gray, D. H., Seach, N., Ueno, T., Milton, M. K., Liston, A., Lew, A. M., Goodnow, C. C., and Boyd, R. L. (2006) *Blood* **108,** 3777–3785

24. Rossi, S., Blazar, B. R., Farrell, C. L., Danilenko, D. M., Lacey, D. L., Weinberg, K. I., Krenger, W., and Holländer, G. A. (2002) *Blood* **100,** 682–691

25. Anderson, M. S., Venanzi, E. S., Klein, L., Chen, Z., Berzins, S. P., Turley, S. J., von Boehmer, H., Bronson, R., Dierich, A., Benoist, C., and Mathis, D. (2002) *Science* **298,** 1395–1401

26. Gray, D. H., Tull, D., Ueno, T., Seach, N., Classon, B. J., Chidgey, A., McConville, M. J., and Boyd, R. L. (2007) *J. Immunol.* **178,** 4956–4965

27. Hay, E. D. (2005) *Dev. Dyn.* **233,** 706–720

28. Iwano, M., Plieth, D., Danoff, T. M., Xue, C., Okada, H., and Neilson, E. G. (2002) *J. Clin. Investig.* **110,** 341–350

29. Mani, S. A., Guo, W., Liao, M. J., Eaton, E. N., Ayyanan, A., Zhou, A. Y., Brooks, M., Reinhard, F., Zhang, C. C., Shipitsin, M., Campbell, L. L., Polyak, K., Brisken, C., Yang, J., and Weinberg, R. A. (2008) *Cell* **133,** 704–715

30. Strutz, F., Okada, H., Lo, C. W., Danoff, T., Carone, R. L., Tomaszewski, J. E., and Neilson, E. G. (1995) *J. Cell Biol.* **130,** 393–405

31. Friedenstein, A. J. (1962) *Nature* **194,** 698–699

32. Kenins, L., Gill, J. W., Boyd, R. L., Holländer, G. A., and Wodnar-Filipowicz, A. (2008) *J. Exp. Med.* **205,** 523–531

33. Anderson, M., Anderson, S. K., and Farr, A. G. (2000) *Int. Immunol.* **12,** 1105–1110

34. van Ewijk, W., Holländer, G., Terhorst, C., and Wang, B. (2000) *Development* (*Camb.*) **127,** 1583–15891

35. Ohbo, K., Suda, T., Hashiyama, M., Mantani, A., Ikebe, M., Miyakawa, K., Moriyama, M., Nakamura, M., Katsuki, M., Takahashi, K., Yamamura, K., and Sugamura, K. (1996) *Blood* **87,** 956–967